Electro-manipulation of droplets for microfluidic applications

L.T. Corson, C. Tsakonas, B.R. Duffy, N.J. Mottram, C.V. Brown and S.K. Wilson

1 Introduction

There is a growing technology-driven interest in using external influences to move or shape small quantities of liquids, referred to as microfluidic actuation. The use of electrical, rather than mechanical, forces to achieve this actuation is convenient because the resultant devices contain no moving parts. Existing non-mechanical microfluidic actuation techniques that are driven by the application of a voltage include electrowetting and liquid dielectrophoresis [9], with many applications including lab-on-a-chip [10], polymer surface patterning [16], as well as optimisation of optical properties for polymer microlenses [12, 20], and droplet driven displays [7].

When an ionic, conducting liquid drop is subjected to a uniform electric field, the drop deforms as a result of the electric stresses on the interface, and it elongates in the direction of the electric field [17]. In this work we consider a sessile drop of an incompressible liquid with a high conductivity resting on the lower plate inside a parallel plate capacitor (Fig.1) subjected to a relatively low frequency A.C. field. This situation is of particular interest to display device applications where the deformation of the drop can be used to change the optical properties of an image pixel [7]. With the application of an electric field the drop deforms into a new static shape where the apex of the drop rises towards the upper plate in order to balance the Maxwell electric stresses, surface tension and hydrostatic pressure due to gravity on the interface. The lower electrode is coated with a thin solid dielectric layer, so the liquid drop is shielded from both electrodes. In this situation the mobile ions will reconfigure to reduce the electric field inside the drop to zero, so that the electric potential of the drop is a constant.

Previous experimental work on the deformation of sessile conductive drops in this geometry has included work on soap bubbles [2], polymer drops [13], water

L. T. Corson, B. R. Duffy, N. J. Mottram, S. K. Wilson, Department of Mathematics & Statistics, University of Strathclyde, 26 Richmond Street, Glasgow G1 1XH, U.K. e-mail: nigel.mottram@strath.ac.uk, · C. Tsakonas, C. V. Brown, School of Science & Technology, Nottingham Trent University, Clifton Lane, Nottingham NG11 8NS, U.K.

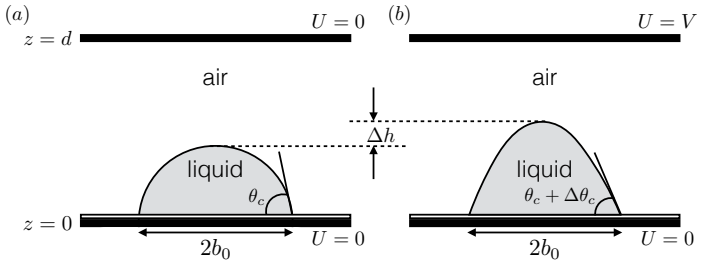

Fig. 1 Sketch of the geometry of a sessile drop resting on the lower plate inside a parallel plate capacitor. The lower electrode is coated with a thin solid dielectric layer. An electric field applied across the capacitor plates deforms the drop (b).

drops in air [3, 6, 14], water drops immersed in dielectric oil [15], and various alcohols in air [4, 5, 18]. As well as different liquids, these experiments also considered different substrate treatments (untreated, hydrophilic and hydrophobic), and therefore the initial contact angles of the drop varied greatly (specifically from from 15 to 160 degrees) [19]. Theoretical work in this geometry has tended to employ numerical techniques to solve the coupled electrostatic and augmented-Young-Laplace equations for the electric field and drop profile. To simplify the process, many authors consider small drops where the assumption of negligible gravity is valid (see e.g. [1, 2, 13]).

In this paper we consider, experimentally and theoretically, the situation of pinned conductive liquid drops with contact angles that are not equal to, but are close to, $\pi/2$. Using both numerical and asymptotic approaches we find solutions to the coupled electrostatic and augmented-Young-Laplace equations which agree very well with the experimental results. Our asymptotic solution for the drop profile extends that of [2] to drops that have initial contact angles close to $\pi/2$ and higher values of the electric field, and provides a predictive equation for the deformation as a function of initial contact angle and drop width, surface tension and applied voltage.

2 Experimental setup

Figure 1 shows the experimental setup. A sessile drop of the liquid trimethylolpropane triglycidyl ether (TMPGE) rests on the lower plate inside a parallel plate capacitor with gap d between the electrodes. TMPGE is often considered a non-conducting dielectric material. However, dielectric studies show that, at the frequencies and voltages used in our experiments, this is a lossy material with a high conductivity that masks the dielectric polarisability so that the liquid is more accurately considered as a conductive liquid. The electrodes were formed from a continuous layer of transparent conductor, indium tin oxide on borosilicate glass slides, and

on the lower plate there is a 1 micron thick layer of the dielectric material SU8, which is coated with a commercial hydrophobic coating to give contact angles close to $\pi/2$. The surface tension of the liquid was found to be 40.5 mN m^{-1} and the value of the density was measured as 1157 kg m^{-3}. In this study A.C. voltages at 1 kHz were used and accurate values for the small height changes in the range 1 to 40 μm were obtained using a 20$\times$ microscope. Experiments were conducted for 8 drops of various sizes with contact angles ranging from 1.50 to 1.62 radians (86.1 to 93.1 degrees) and a range of cell gap to drop radius ratios from 2.45 to 4.21. In all experiments the drop contact line was observed to be pinned with no appreciable movement even at the highest voltages used. Experimental results for the height change at the top of the drop Δh will be shown in §4 when comparisons with numerical solutions of the theoretical model are made.

3 Theoretical model

In our theoretical model an axisymmetric drop of an incompressible, perfectly conductive liquid rests on the lower plate inside a parallel plate capacitor surrounded by a perfect dielectric, in this case air, as shown in Fig. 1. Guided by the experimental results, the contact line of the drop is assumed to be pinned and we take the drop base diameter to be a constant $2b_0$; the contact angle without an electric field applied is denoted by θ_c, while the contact angle with an electric field applied is denoted by $\theta_c + \Delta\theta_c$, where $\Delta\theta_c$ is the electric-field-induced change in the contact angle. The capacitor plates are separated by a distance d, and we assume that the thickness of the dielectric layer on top of the lower electrode is negligible. The electric potential on this lower electrode is therefore assumed to be zero, and at the top electrode the electric potential is equal to V. This is a reasonable approximation given that the thickness of the dielectric layer is small, 1 μm, compared to the other dimensions of our system: b_0 and d are of the order of millimetres.

We use spherical polar coordinates with an origin at the centre of the base of the drop with r being the distance from the origin and θ the angle the radial vector makes with the axis of symmetry. The drop interface is then defined as the zero level of the function $\eta = r - R(\theta)$, so that at any particular angle θ the distance of the interface from the origin is $R(\theta)$.

The drop interface $R(\theta)$ and the electric field $\mathbf{E} = -\nabla U$, where $U(r,\theta)$ is the electric potential, are governed by Laplace's equation and the normal stress balance, often termed the augmented Young–Laplace equation. Since the drop is assumed to be a perfectly conductive liquid, the electric potential inside the drop will be constant, and determined by the proximity of the lower electrode which is fixed at $U = 0$. The upper substrate is held at a potential $U = V$. The boundary conditions for the interface are those of axisymmetry and that the contact line is fixed at $r = b_0$. In addition, the volume of the drop $\mathscr{V}$ is assumed constant, a condition that allows the determination of the drop pressure p.

The governing equations and boundary conditions are made dimensionless by scaling distance by b_0, so that $r = b_0 r^*$ and $R = b_0 R^*$, and by writing

$$\mathscr{V} = \frac{2\pi b_0^3}{3}\mathscr{V}^*, \quad \mathbf{E} = \frac{V}{d}\mathbf{E}^*, \quad U = \frac{V b_0}{d}U^*, \quad p - p_a = \frac{\sigma}{b_0}p^*, \tag{1}$$

and we define a non-dimensional electric Bond number, gravitational Bond number, and scaled cell gap as

$$\delta^2 = \frac{\varepsilon_0 \varepsilon_2 V^2 b_0}{\sigma d^2}, \quad G = \frac{\rho g b_0^2}{\sigma}, \quad D = \frac{d}{b_0}, \tag{2}$$

respectively. Here p_a is the constant air pressure, ρ is the fluid density, σ is the constant surface tension, ε_0 is the permittivity of free space and ε_2 is the relative permittivity of the air, which is approximately equal to one.

Then, with the stars dropped for clarity, the drop interface R and the electric potential U must satisfy

$$\nabla^2 U = \frac{1}{r^2}\frac{\partial}{\partial r}\left(r^2 \frac{\partial U}{\partial r}\right) + \frac{1}{r^2 \sin\theta}\frac{\partial}{\partial \theta}\left(\sin\theta \frac{\partial U}{\partial \theta}\right) = 0, \tag{3}$$

$$p - GR\cos\theta + \delta^2\left((\mathbf{E}\cdot\mathbf{n})^2 - \frac{1}{2}|\mathbf{E}|^2\right) = \nabla\cdot\mathbf{n}, \tag{4}$$

subject to the boundary conditions

$$U(r,\pi/2) = 0, \quad U(r,\theta) = D \quad \text{on} \quad r\cos\theta = D, \quad U(R,\theta) = 0, \tag{5}$$

$$R(\pi/2) = 1, \; R'(0) = 0, \tag{6}$$

and the volume constraint

$$\mathscr{V} = \int_0^{\pi/2} R^3 \sin\theta \; \mathrm{d}\theta = \text{constant}. \tag{7}$$

In order to compare to experimental measurements we consider the height change at the top of the drop, $\Delta h = R(0) - R(0)|_{\delta^2=0}$, where $R(0)|_{\delta^2=0}$ is the initial height of the drop without an electric field applied.

Using this theoretical model of the experimental system we will carry out numerical simulations and compare with the experimental results. Using evidence from these numerical simulations, we can find asymptotic solutions in appropriate limits, although these calculations are only summarised here and will be detailed elsewhere.

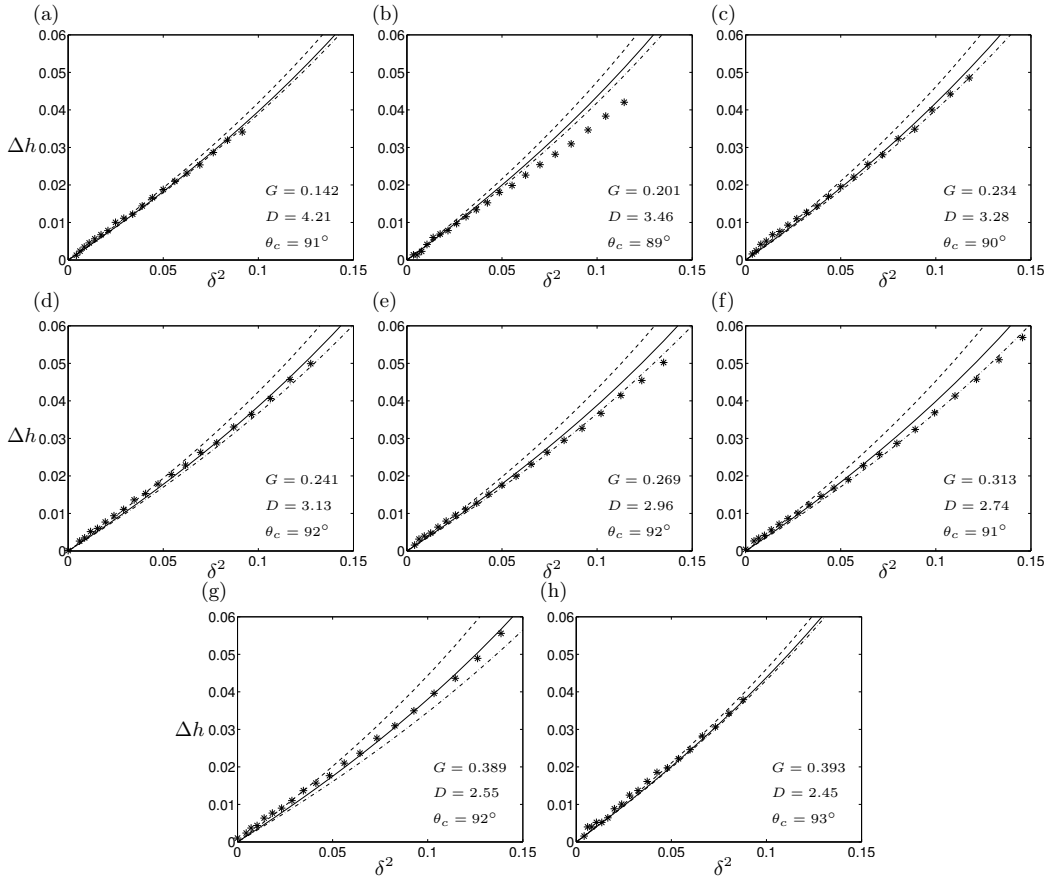

Fig. 2 Change in height at the top of the drop Δh plotted against electric Bond number δ^2 for each experiment (stars) along with the full numerical solution (solid line). Also shown are numerical solutions using two simplifying assumptions: with gravity neglected (dashed line) and with an upper electrode very far from the drop (dash-dotted line).

4 Numerical results and comparison with experimental results

The theoretical model described above was solved numerically using COMSOL [8] and MATLAB [11], where solutions to Laplace's equation (3), subject to (5), and solutions to the normal stress balance (4), subject to (6), are found iteratively until convergence is achieved. Figure 2 compares the experimentally measured change in height at the top of the drop (stars) to the full numerical solution (solid line) for the eight experimental drops. Figure 2 illustrates the validity of the numerical solutions over a range of parameter values: the gravitational Bond number G which increases from panel (a)–(h), the cell gap to drop radius D which decreases from panel (a)–(h),

and the initial contact angle θ_c. We see that there is very good agreement between the experimental results and the numerical solution.

Figure 2 also shows numerical solutions using two simplifying assumptions: with gravity neglected (dashed line) and with the upper electrode very far from the drop (dash-dotted line). We see that, for all values of D we consider, the assumption of infinite cell gap seems valid and there is good agreement between theory and experiments. Unsurprisingly, since $G > 0.1$ for all drops, the numerical solutions with $G = 0$ overestimate the deformation, although the numerical solutions with gravity included do reproduce the experimental results.

From Fig. 2 we see that the deformation may be approximated by $\Delta h = \alpha_{0,2}\delta^2 + \alpha_{1,2}\varepsilon\delta^2 + \alpha_{0,4}\delta^4$, and fitting to the experimental results we find coefficients $\alpha_{0,2} = 0.366 \pm 0.012$, $\alpha_{1,2} = -1.059 \pm 0.419$ and $\alpha_{0,4} = 0.090 \pm 0.096$. For the theoretical model we find the numerically determined coefficients $\alpha_{0,2} = 0.375$, $\alpha_{1,2} = -0.966$ and $\alpha_{0,4} = 0.541$. The experimental coefficients for $\alpha_{0,2}$ and $\alpha_{1,2}$ agree well with the theoretical coeffcients, although the large amount of scatter in experimental values for the $\alpha_{0,4}$ coefficient suggests that the level of noise in the experimentally obtained deformations is of order δ^4.

5 Summary and discussion

In this short paper we have considered, both experimentally and theoretically, pinned liquid drops with contact angles that are close to $\pi/2$. Numerical solutions of the theoretical model agree very well with experimental results for 8 drops with contact angles ranging from 86.1 to 93.1 degrees and cell gap to drop radius ratios from 2.45 to 4.21.

For these experiments it was also noted that the assumption of an infinite cell gap $D \to \infty$ was a good approximation to the experimental situation. Also, although a model with the further simplifying assumption of zero-gravity $G = 0$ did not accurately reproduce the experimental results, the fit to experiments was sufficiently close to consider a simplified model in order to make analytic progress. Therefore, an approximate analysis of the theoretical model, with $G \to 0$ and $D \to \infty$, was undertaken (further details of which will be published elsewhere). For this analysis we obtain,

$$\Delta h = \frac{3}{8}\delta^2 - \left(\frac{1}{4} + \ln 2\right)\varepsilon\delta^2 + \left(\frac{69}{64} - \frac{3}{4}\ln 2\right)\delta^4 = 0.375\delta^2 - 0.943\varepsilon\delta^2 + 0.558\delta^4,$$

which is a very good approximation to the numerically obtained results from the full model, and can readily be extended to all orders. The expressions for Δh that are described in this paper predict a reduction in the leading order deformation at the top of the drop as the contact angle decreases (ε increases). This numerical implementation of the theoretical model, as well as the approximate analytical solution, therefore provide accurate solutions for the drop profile $R(\theta)$ and electric potential

$U(r, \theta)$, and form a useful predictive tool for the electro-manipulation of a conductive sessile drop in a parallel plate capacitor.

References

1. Adamiak, K.: Numerical investigation of shape of liquid droplets in an electric field. In: C.A. Brebbia, S. Kim, T.A. Oswald, H. Power (eds.) Boundary Element XVII, pp. 494–511. Comp. Mech. Publ. (1995)
2. Basaran, O.A., Scriven, L.E.: Axisymmetric shapes and stability of pendant and sessile drops in an electric field. J. Colloid Interface Sci. **140**, 10–30 (1990)
3. Bateni, A., Ababneh, A., Elliott, J.A.W., Neumann, A., Amirfazli, A.: Effect of gravity and electric field on shape and surface tension of drops. Adv. Space. Res. **36**, 64–69 (2005)
4. Bateni, A., Amirfazli, A., Neumann, A.: Effects of an electric field on the surface tension of conducting drops. Colloids Surf., A **289**, 25–38 (2006)
5. Bateni, A., Laughton, S., Tavana, H., Susnar, S., Amirfazli, A., Neumann, A.: Effect of electric fields on contact angle and surface tension of drops. J. Colloid Interface Sci. **283**, 215–222 (2005)
6. Bateni, A., Susnar, S., Amirfazli, A., Neumann, A.: Development of a new methodology to study drop shape and surface tension in electric fields. Langmuir **20**, 7589–7597 (2004)
7. Blankenbach, K., Rawert, J.: Bistable electrowetting displays. Proc. SPIE **7956**, 795,609 (2011)
8. COMSOL Multiphysics: version 4.3b. COMSOL Inc. (2013)
9. Jones, T.B.: Microfluidic schemes using electrical and capillary forces. J. Phys. Conf. Ser. **142**, 012,054 (2008)
10. Kaler, K.V.I.S., Prakas, R., Chugh, D.: Liquid dielectrophoresis and surface microfluidics. Biomicrofluidics **4**, 022,805 (2010)
11. MATLAB: version 8.1 (R2013a). The MathWorks Inc., Natick, Massachusetts (2013)
12. O'Neill, F., Owen, G., Sheridan, J.: Alteration of the profile of ink-jet-deposited UV-cured lenses using applied electric fields. Optik **6**, 158–164 (2005)
13. Reznik, S.N., Yarin, A.L., Theron, A., Zussman, E.: Transient and steady shapes of droplets attached to a surface in a strong electric field. J. Fluid Mech. **516**, 349–377 (2004)
14. Roero, C.: Contact angle measurements of sessile drops deformed by DC electric field. Contact Angle, Wettability and Adhesion, Ed. K. L. Mittal, **4**, 165–176 (2006)
15. Roux, J.M., Achard, J.L., Fouillet, Y.: Forces and charges on an undeformable droplet in the dc field of a plate condenser. J. Electrostatics **66**, 283–293 (2008)
16. Schaffer, E., Thurn-Albrecht, T., Russell, T.P., Steiner, U.: Electrohydrodynamic instabilities in polymer films. Europhys. Lett. **53**, 518–524 (2010)
17. Taylor, G.: Disintegration of water drops in an electric field. Proc. R. Soc. Lond. A **280**(1382), 383–397 (1964)
18. Tsakonas, C., Corson, L., Sage, I.C., Brown, C.V.: Electric field induced deformation of hemispherical sessile drops of ionic liquid. to appear in J. Electrostat. (2014)
19. Vancauwenberghe, V., Di Marco, P., Brutin, D.: Wetting and evaporation of a sessile drop under an external electric field: A review. Colloids Surf. A **432**, 50–56 (2013)
20. Zhan, Z., Wang, K., Yao, H., Cao, Z.: Fabrication and characterization of aspherical lens manipulated by electrostatic field. Appl. Opt. **48**(22), 4375–4380 (2009)